Numerical Calculation and Experimental Validation of RCS Analysis for Radome-Enclosed Scatterer by Using PMCHWT-formulation

***Yoshio Inasawa*[1], *Masayuki Saito*[1], *Izuru Naito*[1], *and Yoshihiko Konishi*[1]**

[1]Mitsubishi Electric Corporation, 5-1-1, Ofuna, Kamakura-shi, Kanagawa, 247-8501, Japan
E-mail: Inasawa.Yoshio@ct.MitsubishiElectric.co.jp

Abstract

This paper investigates the accuracy of RCS analysis for radome-enclosed scatterer by using the PMCHWT-formulation. The analysis method based on a surface integral equation known as the PMCHWT-formulation is outlined shortly. We show that calculated scattering cross section patterns of a dielectric coated conducting sphere agree with exact solutions. Then a RCS pattern of an acrylic hemisphere covered conducting disk is compared with measurement result. Calculated RCS patterns of ellipsoidal radome-enclosed scatterer are also presented. We verify the method of moments using the PMCHWT-formulation is sufficiently accurate for RCS analysis of radome-enclosed scatterer.

1. Introduction

Antennas placed in outdoor environment are generally installed inside a radome to protect them from adverse environmental effects such as wind and rains. Radomes cause a degradation of enclosed antenna performance [1-2] , although the radome wall structure is designed to achieve low transmission loss. Therefore, the radome enclosure have an influence on scattering characteristics of an enclosed scatterer. The effect of radome enclosure should be precisely analyzed in RCS evaluation. Scattering problems of mixed dielectric and conducting objects can be formulated by using a surface integral equation known as the PMCHWT-formulation [3-5]. Scattering characteristics of mixed object are analyzed by solving matrix equation obtained from discretizing and testing the integral equation. The PMCHWT-formulation is widely used to analyze scattering characteristics because it is known to be accurate and free of nonphysical interior resonance problem. It is significant to sufficiently verify the accuracy of the PMCHWT-formulation by numerical calculations and measurements. We compare calculated scattering cross section patterns of a dielectric coated sphere with exact solutions. Then a RCS pattern of an acrylic hemisphere covered conducting disk is compared with measurement result. Calculated RCS patterns of ellipsoidal radome-enclosed scatterer are also presented.

2. Analysis Method

The method of moments using the PMCHWT-formulation is overviewed in this section [3-6]. Let $\mathbf{J}(\mathbf{r}'),\mathbf{M}(\mathbf{r}')$ be equivalent electric and magnetic currents on a closed surface S. Electric and magnetic fields $\mathbf{E}^S(\mathbf{r}),\mathbf{H}^S(\mathbf{r})$ at the observation point $\mathbf{r}$ outside the region S are expressed by

$$\begin{aligned}\mathbf{E}^S(\mathbf{r}) &= -\eta L(\mathbf{J}) + K(\mathbf{M}) \\ \mathbf{H}^S(\mathbf{r}) &= -K(\mathbf{J}) - \eta^{-1} L(\mathbf{M})\end{aligned} \tag{1}$$

where L and K are the following integro-differential operator.

$$\begin{aligned}L(\mathbf{J}) &= jk\left[1+\frac{1}{k^2}\nabla\nabla\cdot\right]\iint_S \mathbf{J}(\mathbf{r}')G(\mathbf{r},\mathbf{r}')d\mathbf{r}' \\ K(\mathbf{J}) &= -\nabla\times\iint_S \mathbf{J}(\mathbf{r}')G(\mathbf{r},\mathbf{r}')d\mathbf{r}' = \iint_S \mathbf{J}(\mathbf{r}')\times\nabla G(\mathbf{r},\mathbf{r}')d\mathbf{r}'\end{aligned} \tag{2}$$

where $G(\mathbf{r},\mathbf{r}')$ is a free space Green's function. Mixed dielectric and conducting objects are shown in Fig. 1. Let $\mathbf{J}_1,\mathbf{M}_1,\mathbf{J}_2,\mathbf{M}_2,\mathbf{J}_3,\mathbf{M}_3$ be equivalent electric and magnetic currents on boundary surfaces S_1 to S_3. Electromagnetic

978-1-4244-6051-9/11/$26.00 ©2011 IEEE

fields $\mathbf{E}^{\text{out}}, \mathbf{H}^{\text{out}}$ outside the boundary S_1 and $\mathbf{E}^{\text{in}}, \mathbf{H}^{\text{in}}$ inside the boundary S_1 is obtained from field equivalent theorem.

$$\begin{aligned}\mathbf{E}^{\text{out}} &= \mathbf{E}^{\text{inc}} - \eta_1 L_1(\mathbf{J}_1) + K_1(\mathbf{M}_1) - \eta_1 L_1(\mathbf{J}_3) + K_1(\mathbf{M}_3) \\ \mathbf{E}^{\text{in}} &= \eta_2 L_2(\mathbf{J}_1) - K_2(\mathbf{M}_1) - \eta_2 L_2(\mathbf{J}_2) + K_2(\mathbf{M}_2)\end{aligned} \tag{3}$$

$$\begin{aligned}\mathbf{H}^{\text{out}} &= \mathbf{H}^{\text{inc}} - K_1(\mathbf{J}_1) - \frac{1}{\eta_1} L_1(\mathbf{M}_1) - K_1(\mathbf{J}_3) - \frac{1}{\eta_1} L_1(\mathbf{M}_3) \\ \mathbf{H}^{\text{in}} &= K_2(\mathbf{J}_1) + \frac{1}{\eta_2} L_2(\mathbf{M}_1) - K_2(\mathbf{J}_2) - \frac{1}{\eta_2} L_2(\mathbf{M}_2)\end{aligned} \tag{4}$$

Here the subscript of the operator indicates the number of each homogeneous region. According to the boundary condition on the surface S_1, the following integral equations are derived by

$$\begin{aligned}&\left[(\eta_1 L_1 + \eta_2 L_2)(\mathbf{J}_1) - (K_1 + K_2)(\mathbf{M}_1) - \eta_2 L_2(\mathbf{J}_2) + K_2(\mathbf{M}_2) + \eta_1 L_1(\mathbf{J}_3) - K_1(\mathbf{M}_3)\right]_{\tan} = \left[\mathbf{E}^{\text{inc}}\right]_{\tan} \\ &\left[(K_1 + K_2)(\mathbf{J}_1) + \left(\frac{1}{\eta_1} L_1 + \frac{1}{\eta_2} L_2\right)(\mathbf{M}_1) - K_2(\mathbf{J}_2) - \frac{1}{\eta_2} L_2(\mathbf{M}_2) + K_1(\mathbf{J}_3) + \frac{1}{\eta_1} L_1(\mathbf{M}_3)\right]_{\tan} = \left[\mathbf{H}^{\text{inc}}\right]_{\tan}\end{aligned} \tag{5}$$

Additional integral equations are derived in the same way by imposing boundary conditions on the surface S_2 and S_3. The matrix equation is obtained from discretizing and testing the PMCHWT-integral equations. The RWG basis function [7] can be used for expansion functions of both electric and magnetic currents. The matrix equation is solved by LU decomposition in the following analysis.

3. Numerical Calculation and Measurement Results

Calculation results are compared with exact solutions to verify the validity of an in-house code based on the method of moments using the PMCHWT-formulation. The analysis model is a dielectric coated conducting sphere shown in Fig. 2. The radii of conducting and dielectric parts are 100mm and 150mm, respectively. The relative permittivity is 2.0 and frequency is 3GHz. Figure 3 shows scattering cross section patterns in the XZ-plane at an incident angle of 0 degrees. The calculation results using the PMCHWT-formulation (indicated by 'MoM') agree with exact solutions in the whole angle range. These results show the validity of the in-house analysis code and the accuracy of the PMCHWT-formulation.

Next a calculated RCS pattern is compared with measurement result. Figure 4 shows a fabricated experimental model of an acrylic hemisphere covered conducting disk. The diameter and thickness of an acrylic hemisphere are 200mm and 2.5mm, respectively. Calculation model is divided into small triangles with a discretization size of 0.1λ at 5GHz and the number of resultant unknowns is 12082. Complex relative permittivity of the acrylic is assumed to be 2.69-j0.2. Figure 5 shows a comparison between calculated and measured RCS patterns. Calculated result almost agrees with measured one, even in the wide angle region. This result shows an effectiveness of the PMCHWT-formulation for RCS analysis of a radome-enclosed scatterer.

Finally we show calculated RCS pattern of an ellipsoidal radome-enclosed conducting disk shown in Fig. 6. The relative permittivity of an ellipsoidal radome is 2.0. Figure 7 shows a calculation model divided into small triangles with a discretization size of 0.1λ at 1GHz. The number of resultant unknowns is 46812. Figure 8 shows a calculated RCS pattern of θ - polarization in the XZ-plane. RCS pattern calculated by Physical Optics (PO) is also shown in this figure. This figure shows the radome enclosure affects RCS pattern of a sole conducting disk. Physical optics dose not predict RCS pattern accurately for a small scatterter. It is significant to analyze the effect of radome enclosure precisely. The method of moments using the PMCHWT-formulation is a promising method for RCS analysis of a radome-enclosed scatterer.

4. Conclusion

We have investigated the accuracy of RCS analysis for radome-enclosed scatterer calculated by the method of moments using the PMCHWT-formulation. Numerical calculation and measurement results of RCS patterns are

presented for a radome-enclosed scatterer. We have verified the method of moments using the PMCHWT-formulation is sufficiently accurate for RCS analysis of a radome-enclosed scatterer.

References

1. G. K. Huddleston and H. L. Bassett, “Radomes,” in R.C. Johnson (ed.), *Antenna Engineering Handbook, Third Edition*, New York, McGraw-Hill, 1992, pp.44-1 - 44-25.
2. M. E. Cooley and D. Davis, “Reflector Antennas,” in M. I. Skolnik (ed.), *Radar Handbook, Third Edition*, New York, McGraw-Hill, 2008, pp.12-39 - 12.41.
3. A. J. Poggio and E. K. Miller, “Integral equation solutions of three dimensional scattering problems,” in R. Mittra (ed.), *Computer Techniques for Electromagnetics*, New York, Pergamon Press, 1973, pp.159 - 264.
4. Y. Chang and R. Harrington, “A surface formulation for characteristic modes of material bodies,” IEEE Trans. Antennas Propag., vol. AP-25, no. 6, Nov. 1977, pp. 789 - 795.
5. T. - K. Wu and L. L. Tsai, “Scattering from arbitrarily-shaped lossy dielectric bodies of revolution,” Radio Sci., vol. 12, no. 5, Sept.-Oct. 1977, pp. 709 - 718.
6. W. C. Chew, J.-M. Jin, E. Michielssen, and J. Song, *Fast and Efficient Algorithms in Computational Electromagnetics*, London, Artech House, 2001, pp. 425 - 460.
7. S. M. Rao, D. R. Wilton, and A. W. Glisson, "Electromagnetic scattering by surfaces of arbitrary shape," IEEE Trans. Antennas and Propag., vol. AP-30, no. 3, May 1982, pp. 409 - 418.

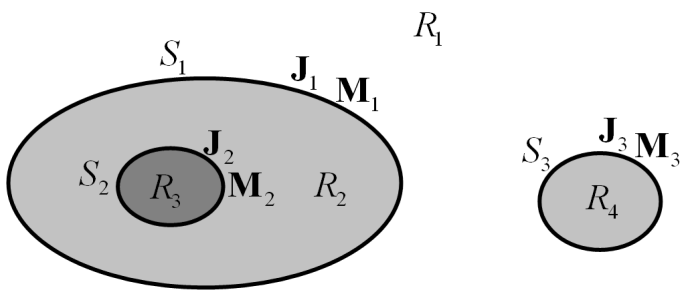

Fig.1 Scattering problem of composite structures.

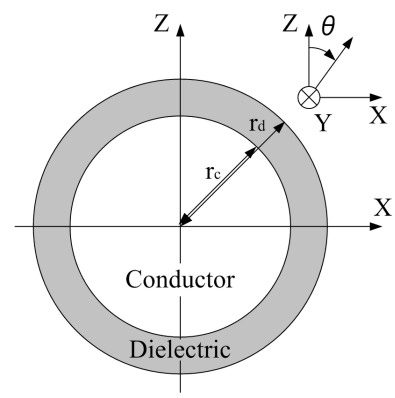

Fig.2 Dielectric coated conducting sphere.

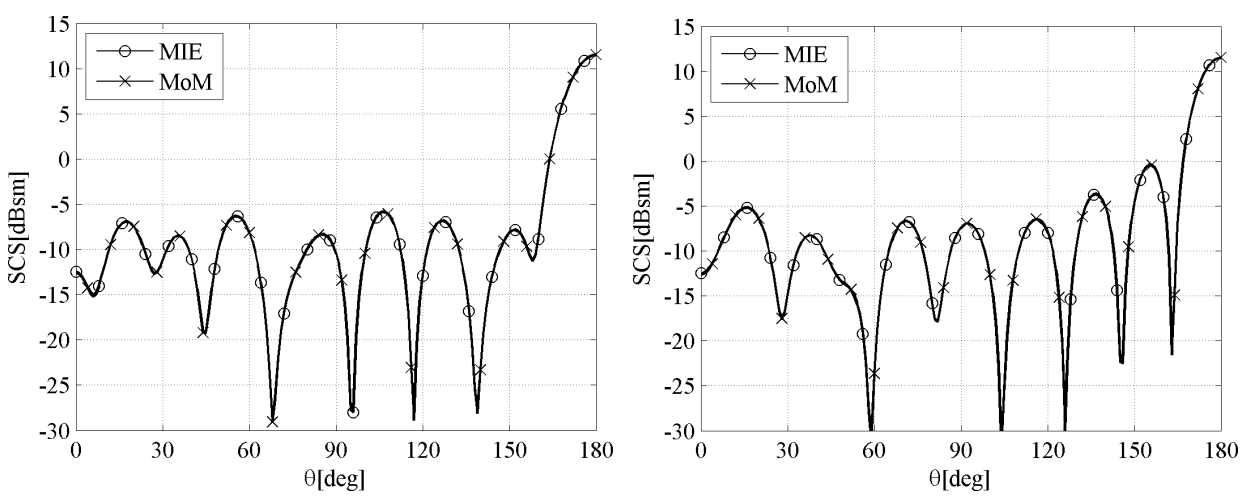

(a) θ - Polarization. (b) ϕ - Polarization.

Fig.3 Scattering characteristics of a dielectric coated conducting sphere.

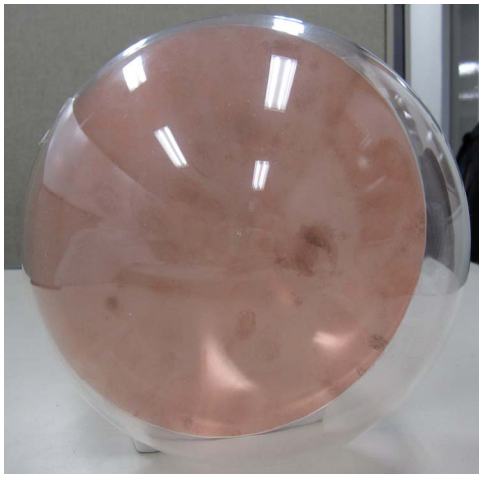

Fig.4 Experimental Model.

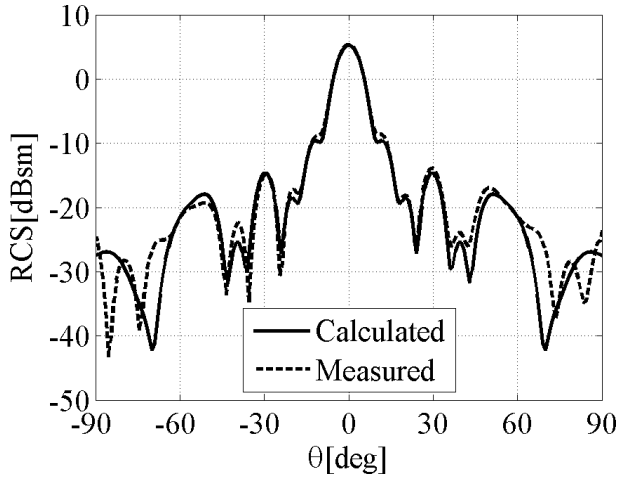

Fig.5 Measurement Result.

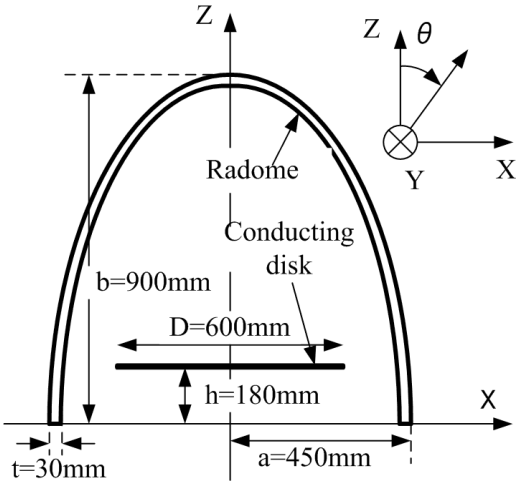

Fig.6 Radome-enclosed conducting disk.

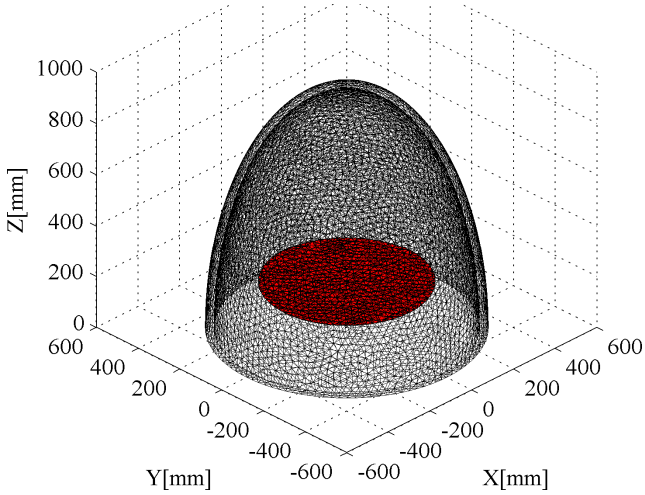

Fig.7 Calculation model.

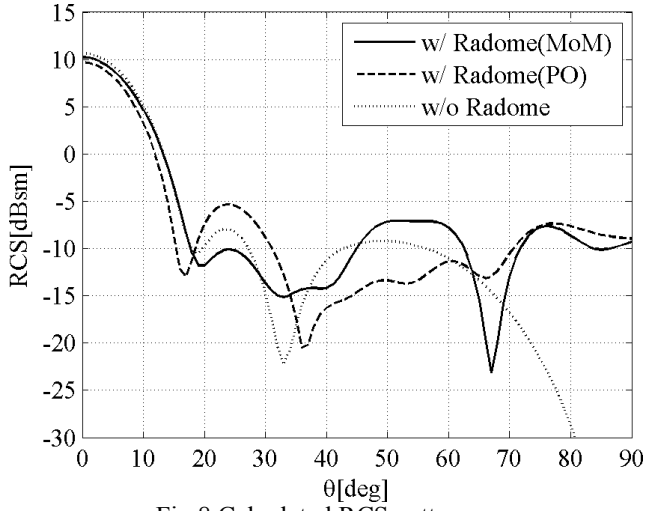

Fig.8 Calculated RCS pattern.